DMD Fast Forward. Published on February 29, 2020 as DOI: 10.1124/dmd.119.089474
This article has not been copyedited and formatted. The final version may differ from this version.

DMD # 89474

**Title**

# Alteration in the plasma concentrations of endogenous OATP1B-biomarkers in non-small cell lung cancer patients treated with paclitaxel

**Authors**

Daiki Mori[1], Hiroo Ishida[2], Tadahaya Mizuno[1], Sojiro Kusumoto[3], Yusuke Kondo[1], Saki Izumi[4], Genki Nakata[1], Yoshitane Nozaki[4], Kazuya Maeda[1], Yasutsuna Sasaki[2], Ken-ichi Fujita[5], Hiroyuki Kusuhara[1]

**Affiliations**

[1] Laboratory of Molecular Pharmacokinetics, Graduate School of Pharmaceutical Sciences, the University of Tokyo, Tokyo, Japan

[2] Division of Medical Oncology, Department of Medicine, Showa University School of Medicine, Tokyo, Japan

[3] Division of Respiratory Medicine and Allergology, Department of Medicine, Showa University School of Medicine, Tokyo, Japan

[4] Drug Metabolism and Pharmacokinetics Tsukuba, Tsukuba Research Laboratories, Eisai Co., Ltd. , Ibaraki, Japan.

[5] Division of Cancer Genome and Pharmacotherapy, Department of Clinical Pharmacy, Showa

DMD Fast Forward. Published on February 29, 2020 as DOI: 10.1124/dmd.119.089474
This article has not been copyedited and formatted. The final version may differ from this version.



University School of Pharmacy, Tokyo, Japan

DMD Fast Forward. Published on February 29, 2020 as DOI: 10.1124/dmd.119.089474
This article has not been copyedited and formatted. The final version may differ from this version.



**Running Title**

Paclitaxel effects on the endogenous OATP1B biomarkers.

**Corresponding Author**

Hiroyuki Kusuhara, Ph.D.

Affiliation: Laboratory of Molecular Pharmacokinetics, Graduate School of Pharmaceutical Sciences,

The University of Tokyo

Address: 7-3-1, Hongo, Bunkyo-ku, Tokyo 113-0033, Japan

Tel: +81-3-5841-4770; Fax: +81-3-5841-4766; Email: kusuhara@mol.f.u-tokyo.ac.jp

**Numbers for manuscript elements**

Text pages:37

Number of tables: 2

Number of figures:5

Number of references:44

Number of Supplemental Tables: 1

Number of Supplemental Figures:11

Number of references in Supplemental Materials:1

DMD Fast Forward. Published on February 29, 2020 as DOI: 10.1124/dmd.119.089474
This article has not been copyedited and formatted. The final version may differ from this version.



Number of words in the Abstract: 226/250

Number of words in the Introduction: 642/750

Number of words in the Discussion: 1421/1,500

**Abbreviations**

AUC, area under the plasma concentration–time curve; C4, 7α-hydroxy-4-cholesten-3-one; CA, cholate; CCK-8, cholecystokinin octapeptide; CPI, coproporphyrin I; CPIII, coproporphyrin III; DDI, drug–drug interaction; E217βG, estradiol 17β glucuronide; GCA, glycocholate; GCDCA, glycochenodeoxycholate; GCDCA-G, glycochenodeoxycholate glucuronide; GCDCA-S, glycochenodeoxycholate sulfate; GDCA, glycodeoxycholate; GDCA-G, glycodeoxycholate glucuronide; GDCA-S, glycodeoxycholate sulfate; GLCA, glycolithocholate; HEK293, human embryonic kidney cells 293; LCA, lithocholate; LC-MS/MS, liquid chromatography-tandem mass spectrometry; OAT, organic anion transporter; OATP, organic anion transporting polypeptide; SEM, standard error of the mean; TCA, taurocholate; TLCA, taurolithocholate

DMD Fast Forward. Published on February 29, 2020 as DOI: 10.1124/dmd.119.089474
This article has not been copyedited and formatted. The final version may differ from this version.



**Abstract**

Paclitaxel has been considered to cause OATP1B-mediated drug–drug interactions at therapeutic doses; however, its clinical relevance has not been demonstrated. This study aimed to elucidate in vivo inhibition potency of paclitaxel against OATP1B1 and OATP1B3 using endogenous OATP1B biomarkers. Paclitaxel is an inhibitor of OATP1B1 and OATP1B3 with $K_i$ of 0.579 ± 0.107 μM and 5.29 ± 3.87 μM, respectively. Preincubation potentiated its inhibitory effect on both OATP1B1 and OATP1B3 with $K_i$ of 0.154 ± 0.031 μM and 0.624 ± 0.183 μM, respectively. Ten non-small cell lung cancer patients who received 200 mg/m$^2$ of paclitaxel by a 3-h infusion were recruited. Plasma concentrations of 10 endogenous OATP1B biomarkers, namely, coproporphyrin I, coproporphyrin III, glycochenodeoxycholate-3-sulfate, glycochenodeoxycholate-3-glucuronide, glycodeoxycholate-3-sulfate, glycodeoxycholate-3-glucuronide, lithocholate-3-sulfate, glycolithocholate-3-sulfate, taurolithocholate-3-sulfate, and chenodeoxycholate-24-glucuronide, were determined in the non-small cell lung cancer patients on the day before paclitaxel administration, and after the end of paclitaxel infusion for 7 hours. Paclitaxel increased the area under the plasma concentration–time curve (AUC) of the endogenous biomarkers 2–4-fold although a few patients did not show any increment in the AUC ratios of lithocholate-3-sulfate, glycolithocholate-3-sulfate, and taurolithocholate-3-sulfate. Therapeutic doses of paclitaxel for the treatment of non-small cell lung cancer (200 mg/m$^2$) will cause significant OATP1B1 inhibition during and at the end of the infusion. This is the first demonstration

DMD Fast Forward. Published on February 29, 2020 as DOI: 10.1124/dmd.119.089474
This article has not been copyedited and formatted. The final version may differ from this version.



that endogenous OATP1B biomarkers could serve as surrogate biomarkers in patients.

**Significance Statement**

Endogenous biomarkers can address practical and ethical issues in elucidating transporter-mediated drug–drug interaction (DDI) risks of anticancer drugs clinically. We could elucidate a significant increment of the plasma concentrations of endogenous OATP1B biomarkers following a 3-h infusion (200 mg/m$^2$) of paclitaxel, a time-dependent inhibitor of OATP1B, in non-small cell lung cancer patients. The endogenous OATP1B biomarkers are useful to assess the possibility of OATP1B-mediated DDIs in patients, and help in appropriate designing dosing schedule to avoid the DDIs.

DMD Fast Forward. Published on February 29, 2020 as DOI: 10.1124/dmd.119.089474
This article has not been copyedited and formatted. The final version may differ from this version.



**Introduction**

Organic anion transporting polypeptides 1B1/*SLCO1B1* (OATP1B1) and 1B3/*SLCO1B3* (OATP1B3) are specifically expressed on the sinusoidal membrane of hepatocytes to mediate the uptake of their substrates from the blood circulation into hepatocytes for further elimination to the bile and metabolism (Maeda, 2015; Patel *et al.*, 2016; Hannah H. Lee and Ho, 2017; McFeely *et al.*, 2019). OATP1B1 and OATP1B3 are multispecific transporters that recognize various anionic drugs and play key roles in the clearance of such drugs. Therefore, OATP1B-mediated drug–drug interactions (DDIs via induction or inhibition) could modulate the pharmacokinetics of drugs, and thereby, their pharmacological effect or toxicity (Maeda, 2015; Patel *et al.*, 2016; Hannah H. Lee and Ho, 2017; Asaumi *et al.*, 2019; McFeely *et al.*, 2019). Regulatory agencies in Japan, the US, and EU strongly recommend pharmaceutical industries in their guidelines to assess the possibility of OATP1B-mediated DDIs with their new chemical entities routinely in vitro, and when the DDI risk predicted is above the regulatory thresholds, clinically.

The principle of DDI prediction is to compare the unbound concentration at the site of DDI and inhibition constants ($K_i$) (Giacomini *et al.*, 2010). However, there is a limitation in the current DDI risk prediction for improvement in preclinical stages to avoid false-positive and -negative predictions (Vaidyanathan *et al.*, 2016). Endogenous biomarkers for drug transporters have emerged as surrogate DDI probes to strengthen the in vitro DDI prediction (Chu *et al.*, 2018; Müller *et al.*, 2018; Rodrigues

*et al.*, 2018). Using the typical drug transporter inhibitors, the magnitude of changes of endogenous biomarkers in the area under the plasma concentration–time curves (AUC), and/or renal clearance have been reported for MATEs, OAT1 and OAT3, and OATP1B1 and OATP1B3. The most important advantage of endogenous biomarkers is that researchers are freed from administration of probe drugs, which could increase the opportunity to assess the DDI risk in humans.

An antimicrotubule agent, paclitaxel, has been used in chemotherapy of various tumors, such as non-small cell lung cancer, breast cancer, and ovarian cancer. The major elimination pathway of paclitaxel from the blood circulation is CYP2C8-mediated metabolism to form 6α-hydroxy paclitaxel (Sonnichsen *et al.*, 1995). DDI with paclitaxel as victim drug has been studied in patients who received clopidogrel, which caused time-dependent inhibition of CYP2C8 (Floyd *et al.*, 2012); patients who received both clopidogrel and paclitaxel exhibited higher incidence of severe paclitaxel neuropathy than those treated with paclitaxel and low-dose aspirin, although the impact on paclitaxel pharmacokinetic parameters remains to be determined (Agergaard *et al.*, 2017). In contrast, paclitaxel was also suggested to inhibit OATP1B based on comparison of in vitro $K_i$ values for OATP1B1 and OATP1B3 with its clinically relevant unbound concentrations (Marada *et al.*, 2015; Murata *et al.*, 2019). However, the clinical relevance of OATP1B inhibition by paclitaxel has not been confirmed because of ethical and practical issues in conducting clinical DDI studies in healthy subjects or patients. We and other groups identified glycochenodeoxycholate-3-sulfate (GCDCA-S) (Takehara *et al.*, 2017,

2018), other sulfated bile acids (Thakare *et al.*, 2017; Mori, Kashihara, *et al.*, 2019; Takehara *et al.*, 2019), coproporphyrin I (CPI) and CPIII (Lai *et al.*, 2016; Barnett *et al.*, 2019), tetradecanedioate and hexadecanedioate (Yee *et al.*, 2016, 2019; Barnett *et al.*, 2019) as endogenous biomarkers for OATP1B1/1B3. Accumulation of clinical data in healthy subjects to support the suitability of these OATP1B-endogenous biomarkers could allow us to evaluate the OATP1B-mediated DDI risks of anticancer drugs in patients.

This study was a clinical study designed to assess the changes in plasma concentrations of such endogenous OATP1B biomarkers in patients with non-small cell lung cancer who received paclitaxel chemotherapy (paclitaxel 200 mg/m$^2$ given intravenously by a 3-h infusion, plus dexamethasone, diphenhydramine and famotidine given 30 min prior to paclitaxel administration). In addition, the patients also received drug therapy for treatment of their complications (Table 1), but there was no drug that was administered to all patients.



## Materials and Methods

### Chemicals

[$^3$H]Estradiol 17 β-D-Glucuronide (E217βG) and [$^3$H]CCK-8 were purchased from PerkinElmer Life and Analytical Sciences (Boston, MA). Authentic compounds including stable isotope-labeled compounds used in this study were all commercially available (**Supplemental Materials**). Other

reagents and organic solvents were of a commercially available analytical grade.

**In vitro transport study using transporter-expressing cells**

HEK293 cells, which were stably transfected with OATP1B1, OATP1B3, OAT1, OAT3, or empty vector, were established previously (Deguchi *et al.*, 2004; Hirano *et al.*, 2004). The transport study was performed according to the previous reports (Deguchi *et al.*, 2004; Hirano *et al.*, 2004). Briefly, HEK293 cells were seeded at $2 \times 10^5$ cells/well in 24-well plate coated with poly-L-lysine (50 mg/L) and poly-L-ornithine (50 mg/L). After 48 h, the medium was substituted by DMEM containing 5 mM sodium butyrate. After 24 h, the transport study was conducted. Cells were washed twice and preincubated with Krebs–Henseleit (KH) buffer at 37°C for 5 min. Then, substrates were added to initiate the uptake. At the designated times, incubation buffer was removed and ice-cold KH buffer was added to terminate the uptake.

To evaluate the inhibition potency of paclitaxel and 6α-hydroxy paclitaxel, either paclitaxel or 6α-hydroxy paclitaxel was added simultaneously with the test substrate. When the time dependence of the inhibitory effect was assessed (shown in **Figure 1 and S8**), cells were preincubated in the presence of paclitaxel or 6α-hydroxy paclitaxel for 15 min. In a separate experiment (shown in **Figure S6A**), cells were preincubated in KH buffer containing paclitaxel for the designated periods (5, 10, 30, 60 min), then washed. After washing, uptake was initiated in the absence of inhibitor. To assess the

duration of the inhibitory effect (shown in **Figure S6B),** cells were preincubated with KH buffer containing paclitaxel for 30 min, incubated with paclitaxel-free KH buffer for designated periods (0, 10, 30, 60 min), then uptake was initiated in the absence of paclitaxel.

For quantification of nonradiolabeled compounds, the cells were collected in Milli-Q water using a scraper and disrupted using a bioruptor (Sonic-bio, Kanagawa, Japan). A 20 μL aliquot was mixed with 60 μL of acetonitrile containing the corresponding internal standard solution. After vortex mixing, the mixtures were centrifuged (20,000*g* for 5 min at 4°C) and the supernatants were used for the following LC-MS/MS analyses. For quantification of the radioactivity, the cells were solubilized with 200 μL 0.2 N NaOH overnight at 4°C and then neutralized with 100 μL 0.4 N HCl. Aliquots of the lysates (200 μL) were transferred to scintillation vials containing a scintillation cocktail (Clear-sol I; Nacalai Tesque, Kyoto, Japan), and the radioactivity was measured in a liquid scintillation counter (LS6000SE, Beckman Instruments, Inc., Fullerton, CA). The protein concentration was determined using the protein assay method of Lowry (Lowry *et al.*, 1951) using bovine serum albumin as the protein standard.

**Western blotting to detect OATP1B1 and OATP1B3 in whole cells and cell surface**

Cells were harvested by cell scraper and collected by centrifugation (12,000*g*, 5 min, 4°C). They were lysed by cell lysis buffer (Cell Signaling, Danvers, MA). The samples were centrifuged at

12,000*g* for 10 min at 4°C, and then, the supernatants were used in the analysis. 4×SDS sample buffer (12% SDS, 25% glycerol, 150 mM Tris-HCl pH 7.0, 0.05% bromophenol blue, 6% β-mercaptoethanol) and 2-mercaptoethanol were added one-fourth and one-thirtieth volume of the sample, respectively, and heated at 60°C for 5 min. Then, the whole cell samples were subjected to western blot analysis.

For cell surface analysis of OATP1B1 and OATP1B3 proteins, cell surface biotinylation was conducted as previously described (Mizuno *et al.*, 2015). Briefly, cells were incubated with NHS-SS-Biotin solution (0.5 mg/mL; Pierce Biotechnology, Inc., Rockford, IL) for 20 min at 4°C and washed using phosphate-buffered saline supplemented with $Ca^{2+}$, $Mg^{2+}$, and 100 mM glycine before preparation of cell lysate with cell lysis buffer (Cell signaling). The cell lysate was mixed with 50 μL streptavidin–agarose (Thermo Fisher Scientific, Waltham, MA) and kept under end-over-end rotation for 2 h at 4°C. After centrifugation at 5,900*g* for 1 min at 4°C, the supernatant was removed. The beads were washed with lysis buffer (50 mM Tris, 150 mM NaCl, 5 mM EDTA, 1% Triton-X 100, pH 7.5) twice, high salt buffer (50 mM Tris, 500 mM NaCl, 5 mM EDTA, 0.1% Triton-X 100, pH 7.5) twice, low salt buffer (50 mM Tris, pH 7.5) once. Biotinylated proteins were eluted with 40 μL loading buffer (Milli-Q water/4× SDS loading buffer/2-mercaptoethanol, 35/4/1) for 1 h at 60°C and obtained specimens were subjected to western blotting analysis.

The specimens were loaded into wells of a 10% SDS–PAGE plate with a 3.75% stacking gel and

subjected to immunoblotting as previously described (Hirano *et al.*, 2004). Immunoreactivity was detected with an ECL Prime Western Blotting Detection Kit (Amersham Biosciences, Piscataway, NJ).

**Clinical study design**

This was a prospective study performed with Japanese non-small cell lung cancer patients who received the first cycle of paclitaxel and carboplatin regimen. To evaluate the difference in plasma concentration profiles of the endogenous substrates with or without the paclitaxel infusion, the blood samples were collected on two consecutive days at the same time points. On day 1, plasma samples were collected before and after the paclitaxel infusion as shown below, while on day 0, plasma samples were collected at the same time points as day 1. The study was conducted in accordance with the principles of the Declaration of Helsinki. This study protocol was approved by the Institutional Review Board of Showa University and Graduate School of Pharmaceutical Sciences, The University of Tokyo. All patients were asked for written informed consent for their peripheral blood samples and medical information to be used for research purposes. The study was registered at the University Hospital Medical Information Network-Clinical Trials Registry Japan (UMIN000032370).

**Eligibility**

DMD Fast Forward. Published on February 29, 2020 as DOI: 10.1124/dmd.119.089474
This article has not been copyedited and formatted. The final version may differ from this version.



All patients 20 years or older with metastatic or recurrent and histologically confirmed non-small cell lung cancer who received paclitaxel, had an Eastern Cooperative Oncology Group performance status of 0–1, and no history of chemotherapy within 4 weeks were eligible. Each patient was confirmed to have adequate bone marrow function (absolute neutrophil count, at least $1.5 \times 10^9$/L; platelet count, at least $150 \times 10^9$/L), liver function (serum bilirubin level, less than 1.5 mg/dL; transaminases, less than 2.5 times the upper limit of normal), and renal function (serum creatinine level, less than 1.5 mg/dL) (**Table 1**).

**Treatment**

The therapeutic dose of paclitaxel (200 mg/m$^2$) and carboplatin (area under the blood concentration–time curve of 6 mg/mL × min) was administered to patients with non-small cell lung cancer. Combination chemotherapy with bevacizumab (15 mg/kg) was permitted. Paclitaxel was administered as an intravenous drip infusion over the course of 3 h after the patient received premedication with oral 50 mg diphenhydramine followed by intravenously given 3 mg granisetron, 50 mg ranitidine, and 20 mg dexamethasone over the course of 10 min (**Figure S1**). Thereafter, carboplatin was given as an intravenous drip infusion over the course of 1 h. The patients were given a dietary supplement containing an equivalent amount of total daily lipids, to minimize the influence of these dietary ingredients on the synthesis or disposition of the

endogenous substrates of OATP1B1 and 1B3 such as bile acids. Note that regular meals were served to patients at 8:00 AM and 12:00 PM with the same menu on day 0 and day 1, and paclitaxel infusion was performed from 11:00 AM to 2:00 PM.

**Blood sampling**

Blood samples were taken from the arm opposite the infusion site at the beginning of paclitaxel infusion and 0, 2, 4, and 7 h after the end of the 3-h infusion of paclitaxel on day 1. Blood samples were also collected at the same time points on day 0 to assess the difference in plasma concentration profiles of the endogenous substrates in the presence or absence of paclitaxel infusion. The blood samples were immediately centrifuged, and the plasma was stored at –80°C until analysis.

**Genotyping of SLCO1B1 in patients**

This study focused on two SLCO1B1 single nucleotide polymorphisms, 388G>A and 521T>C, that form haplotypes, *1a, *1b, and *15. The genotypes were determined as described previously (Akiyama *et al.*, 2012) using genomes prepared from peripheral blood cells of the patients.

**Determination of the unbound fraction of paclitaxel in the plasma**

DMD Fast Forward. Published on February 29, 2020 as DOI: 10.1124/dmd.119.089474
This article has not been copyedited and formatted. The final version may differ from this version.



The unbound fraction of paclitaxel in the plasma ($f_p$) was determined at 0 h and 7 h using a High Throughput Dialysis Model HTD96b and Dialysis Membrane Strips MWCO 12–14 kDa obtained from HTDialysis, LLC (Gales Ferry, CT).

**Quantification of paclitaxel, 6α-hydroxy paclitaxel in the plasma specimens**

Plasma aliquot (20 μL) was added to acetonitrile (180 μL), vortexed, and centrifuged at 20,000*g* for 5 min for protein precipitation. The supernatant (10 μL) was mixed with 0.1% formic acid/acetonitrile = 1/1 solvents (150 μL) and analyzed using LC-MS/MS. Chromatography was performed on a Prominence UFLC system (Shimadzu, Kyoto, Japan) and separation was achieved as described in **Supplemental Methods**. Data were collected on an AB Sciex API5500 (QTRAP) mass spectrometer (Foster City, CA, USA) using positive Turbo IonSpray™ electrospray ionization (ESI) and MRM mode (**Supplemental Methods**). Data acquisition and processing were carried out with Analyst software version 1.6.2. (Applied Biosystems/MDS Sciex, Foster City, Canada).

**Quantification of endogenous OATP1B biomarkers and bile acids in the plasma specimens**

A QTRAP5500 mass spectrometer (AB Sciex, Foster City, Canada) equipped with Prominence UFLC system (Shimadzu, Kyoto, Japan), or Nexera UHPLC (Shimadzu, Kyoto, Japan) was used for quantification of endogenous compounds. Quantification of C4, bile acids, and bile acid sulfates (LCA-S, TLCA-S, and GLCA-S) was performed as described previously (Mori, Kashihara, *et al.*,

DMD Fast Forward. Published on February 29, 2020 as DOI: 10.1124/dmd.119.089474
This article has not been copyedited and formatted. The final version may differ from this version.



2019; Mori, Kimoto, *et al.*, 2019). The measurement method is summarized in **Supplemental Methods**. For separation of stereoisomers, such as CPI and CPIII, GCDCA-S and GDCA-S, and GCDCA-G and GDCA-G, the chromatographic separation was modified as described in the **Supplemental Methods**. The chromatographic separation and analytical condition are described in the **Supplemental Methods**.

**Calculation of AUC of the endogenous compounds**

The area under the plasma concentration–time curve (AUC) was calculated from –3 to 10 h using the linear trapezoidal method using Excel.

**Determination of the inhibition constants ($K_i$) of paclitaxel and 6α-hydroxy paclitaxel for OATP1B1 and OATP1B3**

Iterative nonlinear least-squares method using GraphPad Prism8 (GraphPad Software, San Diego, CA) was conducted to determine the $K_i$ values of paclitaxel or 6α-hydroxy paclitaxel. The uptake of test compound determined in the presence and absence of inhibitor ($CL_{uptake\ (+inhibitor)}$ and $CL_{uptake\ (control)}$, respective) was fitted to the following equation:

$$CL_{uptake(+inhibitor)} = \frac{CL_{uptake(control)}}{1 + I/K_i}$$

where I represents the inhibitor concentration.

**Statistics**

Paired *t*-test was used to examine statistical significance in the effect of paclitaxel administration on the plasma concentrations of endogenous OATP1B biomarkers using GraphPad Prism8 (GraphPad Software, San Diego, CA). Geometric means and 95% confidence of intervals of AUC ratio were calculated using GraphPad Prism8.

**Results**

**Effect of paclitaxel on OATP1B1- and OATP1B3-mediated uptake in HEK293 cells**

Paclitaxel inhibited the OATP1B1-mediated uptake of [$^3$H]E217βG in a concentration-dependent manner (**Figure 1**) with $K_i$ of 0.579 ± 0.107 μM with a competitive manner (**Figure S2**). A 15-min preincubation with paclitaxel potentiated its inhibitory effect, reduced the $K_i$ to 0.154 ± 0.031 μM (**Figure 1**). Paclitaxel showed lower inhibition potency to OATP1B3 than OATP1B1 (**Figure 1**) with the estimated $K_i$ of 0.624 ± 0.183 and 5.29 ± 3.87 μM with or without preincubation, respectively (**Figure 1**). OATP1B1 and OATP1B3 were not inhibited by drugs administered prior to paclitaxel administration (**Figure S3**). Paclitaxel did not inhibit either OAT1 or OAT3 at 10 μM (**Figure S4**).

**Plasma concentration–time profile of paclitaxel in non-small cell lung cancer patients**

Plasma concentrations of paclitaxel and its hydroxy metabolite, 6α-hydroxy paclitaxel, were

determined in the patients (**Figure 2**). Plasma concentrations of 6α-hydroxy paclitaxel accounted for one-tenth of those of paclitaxel (**Figure 2**). The $f_p$ of paclitaxel at 0 h and 7 h were determined in all the subjects. The mean values were 0.0158±0.0042 and 0.0354±0.0247, respectively, which were similar to the previously reported values (0.036~0.079) (Brouwer *et al.*, 2000). The unbound concentration of paclitaxel ($C_{u,max}$) was calculated using individual $f_p$ and $C_{max}$ at 0 h. It was somewhat below the $K_i$ for OATP1B1 with preincubation (**Figure S5**).

**Effect of paclitaxel administration on the plasma concentrations of the endogenous OATP1B biomarkers**

Plasma concentrations of 10 endogenous biomarkers, three porphyrin metabolites (CPI, and CPIII), and bile acid glucuronides or sulfate (GCDCA-S, GCDCA-G, GDCA-S, GDCA-G, LCA-S, GLCA-S, TLCA-S, CDCA-24G), were determined on day 0 (baseline) and day 1 (before and after paclitaxel administration) (**Figure 3**). During the observed time (–3 to 7 h), there was no obvious change in the plasma concentrations on day 0. After a 3-h infusion of paclitaxel, the plasma concentrations of the endogenous biomarkers were higher than the predose level, or baseline (day 0). The time to reach maximum concentration differed among the biomarkers; end of infusion, CPI, CPIII, and CDCA-24G; 0–2 h postinfusion, GCDCA-S, GDCA-S, LCA-S, GLCA-S, TLCA-S; 4 h postinfusion, GCDCA-G and GDCA-G. The increased plasma concentrations did not return to the

corresponding baseline levels by 7 h postinfusion. Note that LCA-S, GLCA-S, and TLCA-S could not be quantified in one patient (PTX-5).

The interindividual difference in the response to paclitaxel administration is shown as AUC in **Figure 4**. The mean and range of the AUC ratio are shown in **Table 2**. There were nonresponders (AUC ratio < 1.25) to paclitaxel for LCA-S, GLCA-S, and TLCA-S; LCA-S, PTX-7 and PTX-10; GLCA-S, PTX-7 and PTX-9; TLCA-S, PTX-7, PTX-8, and PTX-9. Because of these nonresponders, the mean ratio of AUC was somewhat smaller for these metabolites. The mean ratio of AUC was similar among the other metabolites (**Table 2**).

**Effect of paclitaxel administration on the plasma concentrations of the intermediate metabolites of bile acid synthesis and bile acids**

The plasma concentrations of C4 and bile acids were also measured in the patients with or without paclitaxel administration. The plasma concentrations of C4 on day 0 were similar throughout the study, whereas those on day 1 decreased significantly over time (**Figure 5A**). Plasma concentrations of bile acids including the precursor of the glucuronide and sulfate conjugates, such as GCDCA and GDCA, were also determined. The mean values increased at the end of infusion for TCA, GCA, GCDCA, GDCA and TDCA followed by a rapid decline to the baseline levels, whereas there was no difference in the plasma concentrations of CDCA and DCA with and without paclitaxel administration (**Figure**

**5A**). There was a clear interindividual difference in the baseline levels of bile acids, and effect of paclitaxel administration on AUC of bile acids (**Figure 5B**).

## Discussion

DDI risk assessment of anticancer drugs remains mainly limited to in vitro or animal data because to elucidate the clinical relevance of the inhibition at their therapeutic dose ranges is ethically and practically difficult. Paclitaxel is one of the anticancer drugs which were suggested to inhibit OATP1B by conventional prediction method (Marada *et al.*, 2015; Murata *et al.*, 2019). Taking advantage of endogenous biomarkers, circumventing the need for investigators to administer probe drugs, we assessed OATP1B1 and OATP1B3 inhibition potency of paclitaxel at its therapeutic dose for the treatment of non-small lung cancer.

Consistent with previous reports, the in vitro inhibition study showed the concentration-dependent inhibition of OATP1B1 and OATP1B3 by paclitaxel (**Figure 1**). Competitive inhibition was confirmed for OATP1B1 inhibition (**Figure S2**). Whereas, absence of paclitaxel effect on renal organic anion transporters, OAT1 and OAT3 (**Figure S4**) excludes nonspecific effects, at least during the experiments. Furthermore, the inhibition of OATP1B1 and OATP1B3 by paclitaxel was time dependent (**Figure 1; Figure S6**), which had been reported for cyclosporin A (Shitara and Sugiyama, 2017; Tátrai *et al.*, 2019). A metabolite of paclitaxel, 6α-Hydroxy paclitaxel, retained a time-dependent effect on OATP1B1 with similar inhibition potency, whereas it no longer showed time-dependent inhibition of OATP1B3 (**Figure S8**). The time-dependence of OATP1B1 inhibition appears

DMD Fast Forward. Published on February 29, 2020 as DOI: 10.1124/dmd.119.089474
This article has not been copyedited and formatted. The final version may differ from this version.



to be reversible because the activity partially recovered after incubation in the absence of paclitaxel (**Figure S6**). The possibility that paclitaxel treatment decreased the expression of OATP1B1 and OATP1B3 proteins in whole cells and on the cell surface was excluded (**Figure S7**). Shitara and Sugiyama (2017) proposed a *trans*-inhibition model to account for the time-dependent effect of cyclosporin A (Shitara and Sugiyama, 2017). Paclitaxel may also have inhibitory effect on OATP1B1 in the plasma membrane or from the cytosolic compartment, where paclitaxel accumulated during incubation. It is also possible that paclitaxel inhibits the maintenance of the driving force for OATP1B1 and OATP1B3, which has not been identified, or post-translational modifications such as phosphorylation, as has been proposed for other drug transporters (Sprowl *et al.*, 2016). It should be noted that, as pointed out for OATP1B1 (Izumi *et al.*, 2015), the inhibitory effect of paclitaxel for OATP1B3 was substrate dependent; the inhibitory effect of paclitaxel on OATP1B3-mediated [$^3$H]CCK-8 uptake was weaker than that on pitavastatin uptake (**Figure S9**). Careful selection of test OATP1B3 probe is required for conservative DDI risk assessment.

Comparison of the unbound concentration of paclitaxel in the plasma, estimated as the product of $f_p$ and $C_{max}$, with its $K_i$ for OATP1B1 and OATP1B3 (**Figure S5**) suggests that at this dose regimen, paclitaxel inhibits OATP1B1 more potently than OATP1B3. The plasma concentrations of the endogenous OATP1B biomarkers were significantly higher at the end of paclitaxel infusion than the two control values; baselines determined on the day before paclitaxel administration, and values before starting the administration of paclitaxel (confirming the interday difference) (**Figure 3**). The magnitude of changes in CPI concentrations induced by paclitaxel administration was similar to that previously observed in the subjects with OATP1B1 *15 homozygotes (Mori, Kashihara, *et al.*, 2019) and those who received 300 mg rifampicin (Takehara *et al.*, 2018). Previously, the AUC ratio of GCDCA-S (4.3) when 300 mg rifampicin was administered, which was greater than that of CPI (2.3) (Takehara *et al.*, 2018), whereas the AUC ratios of CPI and GCDCA-S were similar in this study

(**Table 2**). Such a difference may arise from the in vivo inhibition potency of OATP1B1 and OATP1B3 between rifampicin and paclitaxel, or disease-related factors. The AUC ratio of LCA-S, GLCA-S, and TLCA-S did not change in 2–3 patients in this study. Such nonresponse of sulfate conjugates of secondary bile acids to OATP1B inhibition was also observed in the rifampicin study (Mori, Kimoto, *et al.*, 2019). The reason for this remains unknown, but using such metabolites as surrogate OATP1B probes should be avoided.

The plasma concentrations of bile acids were also determined on both days. Those on day 1 at some time points were higher than the predose levels (**Figure 5 and Table S1**). One patient who showed a higher AUC ratio of GCDCA (6.8) than others (0.8–1.7) also showed the highest AUC ratio of GCDCA-S (13) and GCDCA-G (6.4) compared with others (2.4–6 and 1.2–3.1, respectively), but the AUC ratio of CPI was similar. Therefore, the AUC ratio of GCDCA-S and GCDCA-G might be influenced not only by OATP1B inhibition but also by the interday variation or effect of paclitaxel and/or the concomitantly administered drug on GCDCA. The possibility that paclitaxel inhibits NTCP can be excluded because of absence of the effect on NTCP-mediated uptake of [$^3$H]taurocholate at 10 μM (data not shown). In addition, C4, an intermediate metabolite of bile acid synthesis from cholesterol, continued to decline on day 1 after paclitaxel administration (**Figure 5**). Paclitaxel therapy might affect bile acid synthesis.

Though in limited patient number, effect of OATP1B1 genotypes (wild-type homozygotes and *15 heterozygotes) and biochemical test results were shown in **Figure S10 and S11**. A nonsynonymous single nucleotide polymorphism (SNP) of OATP1B1 (c. 521T>C, p.Val174Ala) is

well-known to be associated with higher systemic exposure of OATP1B1 substrate drugs (Hannah H Lee and Ho, 2017; Yee *et al.*, 2018). In Japanese people, this mutation is associated in a haplotype (*15) with another nonsynonymous mutation (c. 388A>G, p.Asn130Asp) (Nishizato *et al.*, 2003). Japanese individuals homozygous for the *15 allele showed higher plasma concentrations of CPI and GCDCA-S than homozygotes of reference types and heterozygotes (Mori, Kashihara, *et al.*, 2019). Consistent with our previous report, individuals heterozygous for this mutation did not show any difference in the plasma concentrations of these substrates (**Figure S10**). Whereas, the AUC ratio of CPIII, but not CPI, appeared to be OATP1B1 genotype dependent (**Figure S10**) which required further confirmation in future studies. There was no significant effect of biochemical test results on the AUC ratio of CPI (**Figure S11**), and other test compounds (**data not shown**).

Together with previously reported practices (Lai *et al.*, 2016; Yee *et al.*, 2016; Shen *et al.*, 2017; Takehara *et al.*, 2017, 2018; King-Ahmad *et al.*, 2018; Kunze *et al.*, 2018; Liu *et al.*, 2018; Müller *et al.*, 2018; Cheung *et al.*, 2019), this study provides more convincing evidence to expand application of the endogenous OATP1B biomarkers to assess in vivo OATP1B inhibition under conditions where administration of probe drugs is limited, or under those closer to actual clinical practice. In addition to paclitaxel, mitoxantrone and etoposide were suggested to cause significant inhibition of OATP1B3 (Marada *et al.*, 2015), and tyrosine kinase inhibitors might cause OATP1B1 inhibition via inhibition of phosphorylation (Sprowl *et al.*, 2016). Endogenous OATP1B biomarkers will be able to

demonstrate their clinical relevance in future studies in patients. Whereas the patients generally received drugs other than the potential perpetrator drug to treat their complications, these could have included drugs for which the clinical risk of OATP1B-mediated DDI has not been adequately assessed. In this study, drugs commonly used to treat all patients comprised dexamethasone, diphenhydramine and famotidine, which at least in vitro, did not inhibit OATP1B1 (**Figure S3**), but the possibility of OATP1B-mediated DDIs with these drugs needs to be confirmed in further studies.

The changes in endogenous OATP1B biomarkers induced by perpetrator drugs must be extrapolated to the changes in the AUC of OATP1B substrate drugs to suggest the risk of OATP1B-mediated DDI. An important tool for this purpose is the use of a physiologically based pharmacokinetic (PBPK) model. Yoshikado et al. constructed a PBPK model of CPI that could account for the plasma concentration–time profiles of CPI after rifampicin administration (Yoshikado *et al.*, 2018). Once an appropriate PBPK model has been constructed for paclitaxel, by analogy with that for CPI, it could be used to help estimate the in vivo $K_i$ of paclitaxel for OATP1B that would be required to simulate DDIs between paclitaxel and OATP1B substrate drugs, including in cases using other dose regimens for paclitaxel medication. In addition, because the plasma concentrations of CPI and CPIII showed the most rapid decline after the end of the infusion (within 2 h) of the endogenous substrates tested, PBPK model-based simulation will indicate whether OATP1B1 inhibition by paclitaxel is significant during infusion and for at least 2 h after the end of infusion, which would enable

implementation of an appropriate dosing schedule to avoid significant DDIs.

In conclusion, the present study showed that paclitaxel could inhibit OATP1B1 and OATP1B3 at the dose for the non-small cell lung cancer treatment (200 mg/m$^2$ by a 3-h infusion). This study increases the feasibility of transporter-mediated DDI risk assessment in clinical settings.

DMD Fast Forward. Published on February 29, 2020 as DOI: 10.1124/dmd.119.089474
This article has not been copyedited and formatted. The final version may differ from this version.



**Authorship Contributions**

*Participated in research design*: Ishida, Mizuno, Maeda, Sasaki, Fujita, Kusuhara.

*Conducted experiments*: Mori, Ishida, Kusumoto, Kondo, Izumi, Nakada, Nozaki, Fujita.

Contributed new reagents or analytic tools: None

*Performed data analysis*: Mori, Mizuno, Maeda, Fujita, Kusuhara.

*Wrote or contributed to the writing of the manuscript*: Mizuno, Fujita, Kusuhara.

**References**

Agergaard K, Mau-Sørensen M, Stage TB, Jørgensen TL, Hassel RE, Steffensen KD, Pedersen JW, Milo MLH, Poulsen SH, Pottegård A, Hallas J, Brøsen K, and Bergmann TK (2017) Clopidogrel–Paclitaxel Drug–Drug Interaction: A Pharmacoepidemiologic Study. *Clin Pharmacol Ther* **102**:547–553, Nature Publishing Group.

Akiyama Y, Fujita KI, Ishida H, Sunakawa Y, Yamashita K, Kawara K, Miwa K, Saji S, and Sasaki Y (2012) Association of ABCC2 genotype with efficacy of first-line FOLFIRI in Japanese patients with advanced colorectal cancer. *Drug Metab Pharmacokinet* **27**:325–335.

Asaumi R, Menzel K, Lee W, Nunoya K-I, Imawaka H, Hiroyuki K, and Sugiyama Y (2019) Expanded PBPK Model of Rifampicin for Predicting Interactions with Drugs and an Endogenous Biomarker via Complex Mechanisms including OATP1B Induction. *CPT pharmacometrics Syst Pharmacol*, doi: 10.1002/psp4.12457.

Barnett S, Ogungbenro K, Ménochet K, Shen H, Humphreys WG, and Galetin A (2019) Comprehensive evaluation of the utility of 20 endogenous molecules as biomarkers of OATP1B inhibition compared with rosuvastatin and coproporphyrin I. *J Pharmacol Exp Ther* **368**:125–135, American Society for Pharmacology and Experimental Therapy.

Brouwer E, Verweij J, De Bruijn P, Loos WJ, Pillay M, Buijs D, and Sparreboom A (2000) Measurement of fraction unbound paclitaxel in human plasma. *Drug Metab Dispos* **28**:1141–5.

Cheung KWK, Yoshida K, Cheeti S, Chen B, Morley R, Chan IT, Sahasranaman S, and Liu L (2019) GDC-0810 Pharmacokinetics and Transporter-Mediated Drug Interaction Evaluation with an Endogenous Biomarker in the First-in-Human, Dose Escalation Study. *Drug Metab Dispos* **47**:966–973, American Society for Pharmacology & Experimental Therapeutics (ASPET).

Chu X, Liao M, Shen H, Yoshida K, Zur AA, Arya V, Galetin A, Giacomini KM, Hanna I, Kusuhara H, Lai Y, Rodrigues D, Sugiyama Y, Zamek-Gliszczynski MJ, and Zhang L (2018) Clinical Probes and Endogenous Biomarkers as Substrates for Transporter Drug-Drug Interaction Evaluation: Perspectives From the International Transporter Consortium. *Clin Pharmacol Ther* **104**:836–864, Nature Publishing Group.

Deguchi T, Kusuhara H, Takadate A, Endou H, Otagiri M, and Sugiyama Y (2004) Characterization of uremic toxin transport by organic anion transporters in the kidney. *Kidney Int* **65**:162–174.

Floyd JS, Kaspera R, Marciante KD, Weiss NS, Heckbert SR, Lumley T, Wiggins KL, Tamraz B, Kwok PY, Totah RA, and Psaty BM (2012) A screening study of drug-drug interactions in cerivastatin users: An adverse effect of clopidogrel. *Clin Pharmacol Ther* **91**:896–904.

Giacomini KM, Huang S, Tweedie DJ, and Benet LZ (2010) Membrane transporters in drug development. The International Transpporter Consortium. *Nat Re Drug Discov* **9**:215–236.

Hirano M, Maeda K, Shitara Y, and Sugiyama Y (2004) Contribution of OATP2 (OATP1B1) and OATP8 (OATP1B3) to the hepatic uptake of pitavastatin in humans. *J Pharmacol Exp Ther*

**311**:139–46.

Izumi S, Nozaki Y, Maeda K, Komori T, Takenaka O, Kusuhara H, and Sugiyama Y (2015) Investigation of the impact of substrate selection on in vitro organic anion transporting polypeptide 1B1 inhibition profiles for the prediction of drug-drug interactions. *Drug Metab Dispos* **43**:235–247.

King-Ahmad A, Clemens S, Ramanathan R, Zhang Yanhua, Raha N, Zhang Yizhong, Holliman C, Rodrigues AD, and Li F (2018) A fully automated and validated human plasma LC-MS/MS assay for endogenous OATP biomarkers coproporphyrin-I and coproporphyrin-III. *Bioanalysis* **10**:691–701, Future Medicine Ltd.

Kunze A, Ediage EN, Dillen L, Monshouwer M, and Snoeys J (2018) Clinical Investigation of Coproporphyrins as Sensitive Biomarkers to Predict Mild to Strong OATP1B-Mediated Drug–Drug Interactions. *Clin Pharmacokinet* **57**:1559–1570, Springer International Publishing.

Lai Y, Mandlekar S, Shen H, Holenarsipur VK, Langish R, Rajanna P, Murugesan S, Gaud N, Selvam S, Date O, Cheng Y, Shipkova P, Dai J, Humphreys WG, and Marathe P (2016) Coproporphyrins in Plasma and Urine Can Be Appropriate Clinical Biomarkers to Recapitulate Drug-Drug Interactions Mediated by Organic Anion Transporting Polypeptide Inhibition. *J Pharmacol Exp Ther* **358**:397–404.

Lee Hannah H, and Ho RH (2017) Interindividual and interethnic variability in drug disposition: polymorphisms in organic anion transporting polypeptide 1B1 (OATP1B1; SLCO1B1). *Br J Clin*

*Pharmacol* **83**:1176–1184.

Lee Hannah H., and Ho RH (2017) Interindividual and interethnic variability in drug disposition: polymorphisms in organic anion transporting polypeptide 1B1 (OATP1B1; SLCO1B1). *Br J Clin Pharmacol* **83**:1176–1184, Blackwell Publishing Ltd.

Liu L, Cheeti S, Yoshida K, Choo E, Chen E, Chen B, Gates M, Singel S, Morley R, Ware J, and Sahasranaman S (2018) Effect of OATP1B1/1B3 Inhibitor GDC-0810 on the Pharmacokinetics of Pravastatin and Coproporphyrin I/III in Healthy Female Subjects. *J Clin Pharmacol* **58**:1427–1435, Blackwell Publishing Inc.

Lowry O, Rosebrough N, Farr A, and Randall R (1951) Protein measurement with the Folin phenol reagent. *J Biol Chem* **193**:265–75.

Maeda K (2015) Organic anion transporting polypeptide (OATP)1B1 and OATP1B3 as important regulators of the pharmacokinetics of substrate drugs. *Biol Pharm Bull* **38**:155–168, Pharmaceutical Society of Japan.

Marada VVVR, Flörl S, Kühne A, Burckhardt G, and Hagos Y (2015) Interaction of human organic anion transporter transporting polypeptides 1B1 and 1B3 with antineoplastic compounds. *Eur J Med Chem* **92**:723–731, Elsevier Masson SAS.

McFeely SJ, Ritchie TK, Yu J, Nordmark A, Levy RH, and Ragueneau-Majlessi I (2019) Identification and Evaluation of Clinical Substrates of Organic Anion Transporting Polypeptides 1B1 and 1B3.

*Clin Transl Sci* **12**:379–387.

Mizuno T, Hayashi H, and Kusuhara H (2015) Cellular Cholesterol Accumulation Facilitates Ubiquitination and Lysosomal Degradation of Cell Surface-Resident ABCA1. *Arterioscler Thromb Vasc Biol* **35**:1347–1356.

Mori D, Kashihara Y, Yoshikado T, Kimura M, Hirota T, Matsuki S, Maeda K, Irie S, Ieiri I, Sugiyama Y, and Kusuhara H (2019) Effect of OATP1B1 genotypes on plasma concentrations of endogenous OATP1B1 substrates and drugs, and their association in healthy volunteers. *Drug Metab Pharmacokinet* **34**:78–86.

Mori D, Kimoto E, Rago B, Kondo Y, King-Ahmad A, Ramanathan R, Wood LS, Johnson JG, Le VH, Vourvahis M, Rodrigues AD, Muto C, Furihata K, Sugiyama Y, and Kusuhara H (2019) Dose-Dependent Inhibition of OATP1B by Rifampicin in Healthy Volunteers: Comprehensive Evaluation of Candidate Biomarkers and OATP1B Probe Drugs. *Clin Pharmacol Ther*, doi: 10.1002/cpt.1695.

Müller F, Sharma A, König J, and Fromm MF (2018) Biomarkers for In Vivo Assessment of Transporter Function. *Pharmacol Rev* **70**:246–277.

Murata H, Ito S, Kusuhara H, Nomura Y, and Taniguchi T (2019) Proposal of a Parameter for OATP1B1 Inhibition Screening at the early Drug Discovery Stage. *J Pharm Sci*, doi: 10.1016/j.xphs.2019.08.012.

Nishizato Y, Ieiri I, Suzuki H, Kimura M, Kawabata K, Hirota T, Takane H, Irie S, Kusuhara H, Urasaki

Y, Urae A, Higuchi S, Otsubo K, and Sugiyama Y (2003) Polymorphisms of OATP-C (SLC21A6) and OAT3 (SLC22A8) genes: consequences for pravastatin pharmacokinetics. *Clin Pharmacol Ther* **73**:554–65.

Patel M, Taskar KS, and Zamek-Gliszczynski MJ (2016) Importance of Hepatic Transporters in Clinical Disposition of Drugs and Their Metabolites. *J Clin Pharmacol* S23–S39, Blackwell Publishing Inc.

Rodrigues AD, Taskar KS, Kusuhara H, and Sugiyama Y (2018) Endogenous Probes for Drug Transporters: Balancing Vision With Reality. *Clin Pharmacol Ther* **103**:434–448, Nature Publishing Group.

Shen H, Chen W, Drexler DM, Mandlekar S, Holenarsipur VK, Shields EE, Langish R, Sidik K, Gan J, Humphreys WG, Marathe P, and Lai Y (2017) Comparative evaluation of plasma bile acids, dehydroepiandrosterone sulfate, hexadecanedioate, and tetradecanedioate with coproporphyrins I and III as markers of OATP inhibition in healthy subjects. *Drug Metab Dispos* **45**:908–919.

Shitara Y, and Sugiyama Y (2017) Preincubation-dependent and long-lasting inhibition of organic anion transporting polypeptide (OATP) and its impact on drug-drug interactions. *Pharmacol Ther* **177**:67–80.

Sonnichsen DS, Liu Q, Schuetz EG, Schuetz JD, Pappo A, and Relling M V (1995) Variability in human cytochrome P450 paclitaxel metabolism. *J Pharmacol Exp Ther* **275**:566–75.

Sprowl JA, Ong SS, Gibson AA, Hu S, Du G, Lin W, Li L, Bharill S, Ness RA, Stecula A, Offer SM,

Diasio RB, Nies AT, Schwab M, Cavaletti G, Schlatter E, Ciarimboli G, Schellens JHM, Isacoff EY, Sali A, Chen T, Baker SD, Sparreboom A, and Pabla N (2016) A phosphotyrosine switch regulates organic cation transporters. *Nat Commun* **7**:10880.

Takehara I, Terashima H, Nakayama T, Yoshikado T, Yoshida M, Furihata K, Watanabe N, Maeda K, Ando O, Sugiyama Y, and Kusuhara H (2017) Investigation of Glycochenodeoxycholate Sulfate and Chenodeoxycholate Glucuronide as Surrogate Endogenous Probes for Drug Interaction Studies of OATP1B1 and OATP1B3 in Healthy Japanese Volunteers. *Pharm Res* **34**:1601–1614.

Takehara I, Watanabe N, Mori D, Ando O, and Kusuhara H (2019) Effect of Rifampicin on the Plasma Concentrations of Bile Acid-O-Sulfates in Monkeys and Human Liver-Transplanted Chimeric Mice With or Without Bile Flow Diversion. *J Pharm Sci* **108**:2756–2764.

Takehara I, Yoshikado T, Ishigame K, Mori D, Furihata K, Watanabe N, Ando O, Maeda K, Sugiyama Y, and Kusuhara H (2018) Comparative Study of the Dose-Dependence of OATP1B Inhibition by Rifampicin Using Probe Drugs and Endogenous Substrates in Healthy Volunteers. *Pharm Res* **35**:138.

Tátrai P, Schweigler P, Poller B, Domange N, de Wilde R, Hanna I, Gáborik Z, and Huth F (2019) A Systematic In Vitro Investigation of the Inhibitor Preincubation Effect on Multiple Classes of Clinically Relevant Transporters. *Drug Metab Dispos* **47**:768–778.

Thakare R, Gao H, Kosa RE, Bi Y-A, Varma MVS, Cerny MA, Sharma R, Kuhn M, Huang B, Liu Y, Yu

A, Walker GS, Niosi M, Tremaine L, Alnouti Y, and Rodrigues AD (2017) Leveraging of Rifampicin-Dosed Cynomolgus Monkeys to Identify Bile Acid 3-O-Sulfate Conjugates as Potential Novel Biomarkers for Organic Anion-Transporting Polypeptides. *Drug Metab Dispos* **45**:721–733.

Vaidyanathan J, Yoshida K, Arya V, and Zhang L (2016) Comparing Various In Vitro Prediction Criteria to Assess the Potential of a New Molecular Entity to Inhibit Organic Anion Transporting Polypeptide 1B1. *J Clin Pharmacol* S59–S72, Blackwell Publishing Inc.

Yee SW, Brackman DJ, Ennis EA, Sugiyama Y, Kamdem LK, Blanchard R, Galetin A, Zhang L, and Giacomini KM (2018) Influence of Transporter Polymorphisms on Drug Disposition and Response: A Perspective From the International Transporter Consortium. *Clin Pharmacol Ther* **104**:803–817.

Yee SW, Giacomini MM, Hsueh CH, Weitz D, Liang X, Goswami S, Kinchen JM, Coelho A, Zur AA, Mertsch K, Brian W, Kroetz DL, and Giacomini KM (2016) Metabolomic and Genome-wide Association Studies Reveal Potential Endogenous Biomarkers for OATP1B1. *Clin Pharmacol Ther* **100**:524–536, Nature Publishing Group.

Yee SW, Giacomini MM, Shen H, Humphreys WG, Horng H, Brian W, Lai Y, Kroetz DL, and Giacomini KM (2019) Organic Anion Transporter Polypeptide 1B1 Polymorphism Modulates the Extent of Drug–Drug Interaction and Associated Biomarker Levels in Healthy Volunteers. *Clin Transl Sci*, doi: 10.1111/cts.12625, Blackwell Publishing Ltd.

Yoshikado T, Toshimoto K, Maeda K, Kusuhara H, Kimoto E, Rodrigues AD, Chiba K, and Sugiyama Y

(2018) PBPK Modeling of Coproporphyrin I as an Endogenous Biomarker for Drug Interactions Involving Inhibition of Hepatic OATP1B1 and OATP1B3. *CPT Pharmacometrics Syst Pharmacol* **7**:739–747.

**Footnotes**

Grants-in-Aid for Scientific Research foundation B from the Japan Society for the Promotion of Science [17H04100]

Grants-in-Aid for Clinical Pharmacology Research Foundation.

**Legends for Figures**

**Figure 1 Inhibitory effect of paclitaxel on the OATP1B1- and OATP1B3-mediated uptake in HEK293 cells.**

The uptake of [$^3$H]E217βG by HEK293 cells stably expressing OATP1B1 and that of pitavastatin (0.3 μM) by HEK293 cells stably expressing OATP1B3 for 3 min with (○) or without (●) paclitaxel preincubation (15 min) was determined in the absence and presence of paclitaxel at the designated concentrations or rifampicin (20 μM). The solid line represents the fitted line obtained by nonlinear regression analysis as described in the *Materials and Methods* section. The dotted line represents the mean value of the uptake of [$^3$H]E217βG in the presence of rifampicin. Each symbol represents the mean value with SEM ($n$ = 3).

**Figure 2 Plasma concentrations of paclitaxel and 6α-hydroxy paclitaxel.**

Plasma concentrations of paclitaxel (closed symbols) and 6α-hydroxy paclitaxel (open symbols) were determined at designated time points in non-small cell lung cancer patients following a 3 h intravenous infusion of paclitaxel (200 mg/m$^2$) from -3h to 0h. Each symbol represents the mean value, and error bars representing SEM ($n$ = 10) were within the symbol.

**Figure 3 Effect of paclitaxel on the plasma concentrations of endogenous OATP1B substrates.**

Plasma concentrations of CPI, CPIII, sulfate-conjugated bile acids (GCDCA-S, GDCA-S, LCA-S, GLCA-S, TLCA-S), and glucuronide-conjugated bile acids (GCDCA-G, GDCA-G, CDCA-24G) were determined at designated time points in non-small cell lung cancer patients treated with or without an intravenous dose of paclitaxel (200 mg/m$^2$). Each symbol represents the mean value, and error bars represent SEM ($n$ = 10). *p < 0.05, **p < 0.01, ***p < 0.001.

**Figure 4 Area under the plasma concentration–time curves for endogenous OATP1B substrates with and without paclitaxel administration**

The symbols represent AUC values in 10 patients calculated using the linear trapezoidal rule from time –3 to 7 h. *p < 0.05, **p < 0.01, ***p < 0.001.

**Figure 5 Plasma concentrations of C4 and bile acids with and without paclitaxel administration.**

(A) Plasma concentrations of C4 and bile acids were determined at designated time points in non-small cell lung cancer patients treated with or without an intravenous dose of paclitaxel (200 mg/m$^2$). Each symbol represents the mean value, and error bars represent SEM ($n$ = 10). *p < 0.05, **p < 0.01, ***p < 0.001.

(B) Area under the plasma concentration–time curves for C4 and bile acids. The symbols represent

individual values of AUC calculated using the trapezoidal rule from time –3 to 7 h. *$p < 0.05$, **$p < 0.01$

**Table 1 Non-small cell lung cancer patient information**



Patient information is summarized in the table. In subject PTX-6, paclitaxel administration was discontinued due to paclitaxel allergy.

| ID | Sex | Age (years) | Height (cm) | Body Weight (kg) | OATP1B1 haplotype | Alb (g/dL) | AGP (mg/dL) | AST (IU/L) | ALT (IU/L) | LDH (IU/L) | ALP (IU/L) | T-Bil (mg/dL) | D-Bil (mg/dL) | SCr (mg/dL) | eGFR (mL/min) | Complications | Medications |
|---|---|---|---|---|---|---|---|---|---|---|---|---|---|---|---|---|---|
| PTX-1 | M | 74 | 159.5 | 54.3 | *1b/*1b | 4.3 | 52.0 | 37 | 21 | 200 | 354 | 1.3 | 0.1 | 0.81 | 71.0 | Alcoholic hepatitis, hyperuricemia, allergic rhinitis | Livact, Feburic, Xyzal |
| PTX-2 | F | 75 | 161.5 | 56.9 | *1a/*1b | 4.0 | 65.0 | 21 | 14 | 180 | 216 | 0.9 | <0.1 | 0.68 | 63.3 | Dyslipidemia, osteoporosis | Lipitor, Edirol, Protecadin |
| PTX-3 | M | 58 | 169 | 73.2 | *1b/*1b | 3.3 | 144.0 | 32 | 24 | 269 | 216 | 0.5 | <0.1 | 0.89 | 68.7 | Hypertension, atrial fibrillation | Tenormin, Atelec, Olmetec, Xarelto, Tambocor, Eperisone, alprazolam |
| PTX-4 | M | 57 | 164.5 | 53.5 | *1b/*15 | 4.2 | 73.0 | 12 | 6 | 115 | 135 | 1.6 | 0.1 | 0.72 | 87.1 | Dyslipidemia | Bezatol, Urso, Pinellia Heart-Purging Decoction, Clostridium butyricum |
| PTX-5 | M | 48 | 169 | 58.6 | *1b/*15 | 4.0 | 76.0 | 28 | 25 | 162 | - | 0.9 | 0.1 | 0.89 | 72.9 | Hypertension | Preminent, Depas |
| PTX-7 | M | 66 | 165 | 63 | *1b/*15 | 3.9 | 84.0 | 35 | 49 | 294 | 305 | 0.5 | 0.1 | 1.03 | 56.4 | Hypertension, angina | Herbesser R, valsartan |
| PTX-8 | M | 67 | 163.5 | 44.6 | *1a/*1b | 3.4 | 154.0 | 19 | 8 | 289 | - | 0.7 | 0.1 | 0.69 | 87.1 | Hypertension | Irbetan, famotidine |
| PTX-9 | M | 57 | 171 | 72 | *1a/*1b | 4.4 | 96.0 | 18 | 13 | 219 | 219 | 0.8 | 0.1 | 0.76 | 82.1 | Hyperuricemia | Alositol, Takecab, Rebamipide |
| PTX-10 | M | 68 | 170 | 63.9 | *1b/*1b | 3.9 | 188.0 | 16 | 9 | 344 | 416 | 0.4 | <0.1 | 1.15 | 49.6 | Reflux esophagitis | Nexium |
| PTX-11 | M | 52 | 160 | 53 | *1a/*1b | 3.7 | 156.0 | 16 | 10 | 156 | 225 | 0.5 | <0.1 | 0.82 | 77.6 | – | Takecab, loxoprofen, Tapenta, Etizolam, Rivotril |

DMD Fast Forward. Published on February 29, 2020 as DOI: 10.1124/dmd.119.089474
This article has not been copyedited and formatted. The final version may differ from this version.

**Table 2 Effect of paclitaxel on $AUC_{-3-7h}$ of Endogenous OATP1B Substrates**

$AUC_{-3-7h}$ of the endogenous OATP1B substrates were calculated. $AUC_{-3-7r}$ are presented as mean ± SEM. Fold changes are presented as GMR and 90% CI. ($n$ = 10).

| Compounds | | Control | + Paclitaxel | Fold change |
|---|---|---|---|---|
| CPI | (nM × h) | 22.1 ± 1.7 | 61.4 ± 4.3 | 2.8 (2.5, 3.1) |
| CPIII | (nM × h) | 4.48 ± 0.34 | 14.1 ± 1.3 | 3.1 (2.6, 3.7) |
| GCDCA-S | (μM × h) | 2.06 ± 0.45 | 5.71 ± 1.0 | 2.9 (2.2, 3.9) |
| GDCA-S | (μM × h) | 0.501 ± 0.09 | 2.2 ± 0.45 | 4.0 (2.8, 5.8) |
| LCA-S | (μM × h) | 0.694 ± 0.16 | 1.46 ± 0.38 | 2.0 (1.2, 3.5) |
| GLCA-S | (μM × h) | 4.15 ± 1.4 | 10.4 ± 3.3 | 2.2 (1.4, 3.6) |
| TLCA-S | (μM × h) | 0.857 ± 0.22 | 1.94 ± 0.57 | 2.0 (1.3, 3.0) |
| GCDCA-G | (nM × h) | 20.6 ± 4.1 | 52.2 ± 10 | 2.5 (1.8, 3.4) |
| GDCA-G | (nM × h) | 94.4 ± 29 | 211 ± 46 | 2.5 (1.8, 3.4) |
| CDCA-24G | (nM × h) | 141 ± 33 | 369 ± 79 | 3.0 (2.2, 4.0) |

# Figure 1

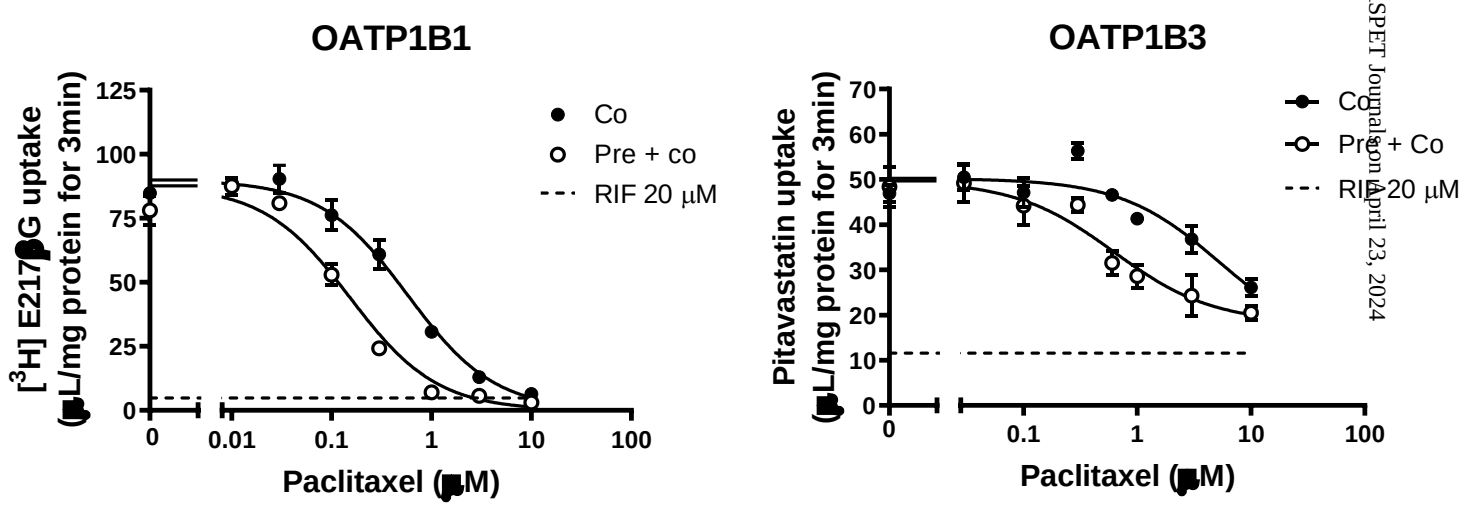

**Figure 2**

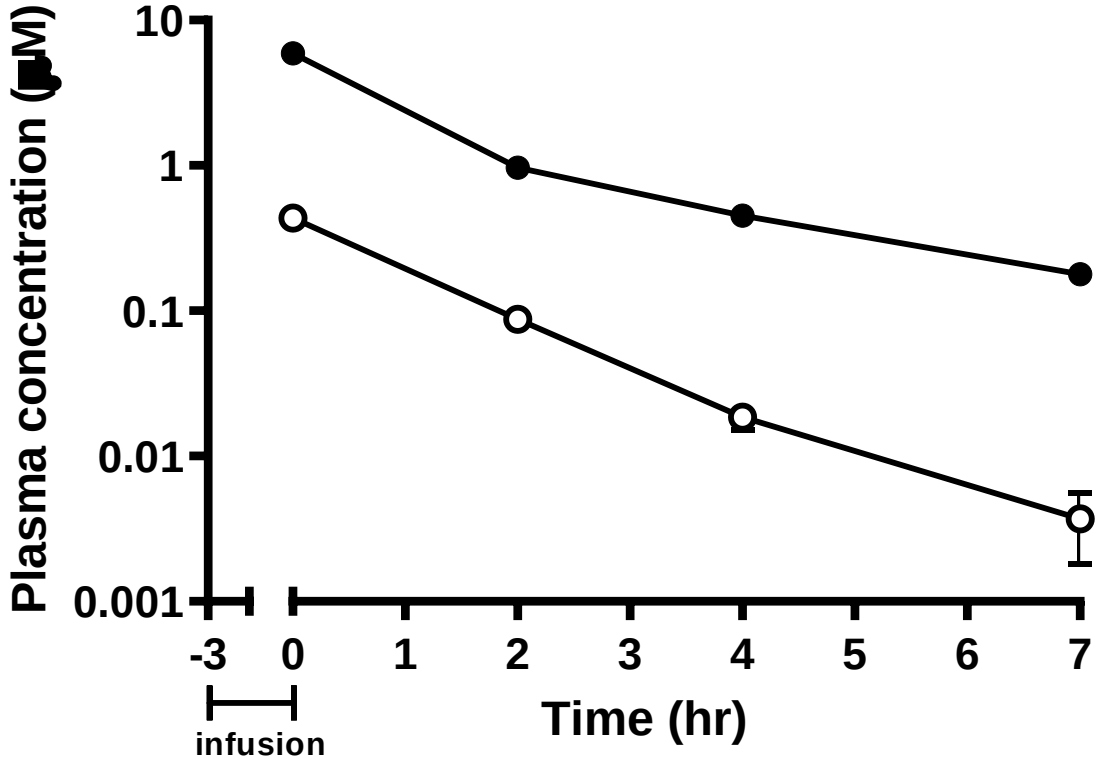

**Figure 3**

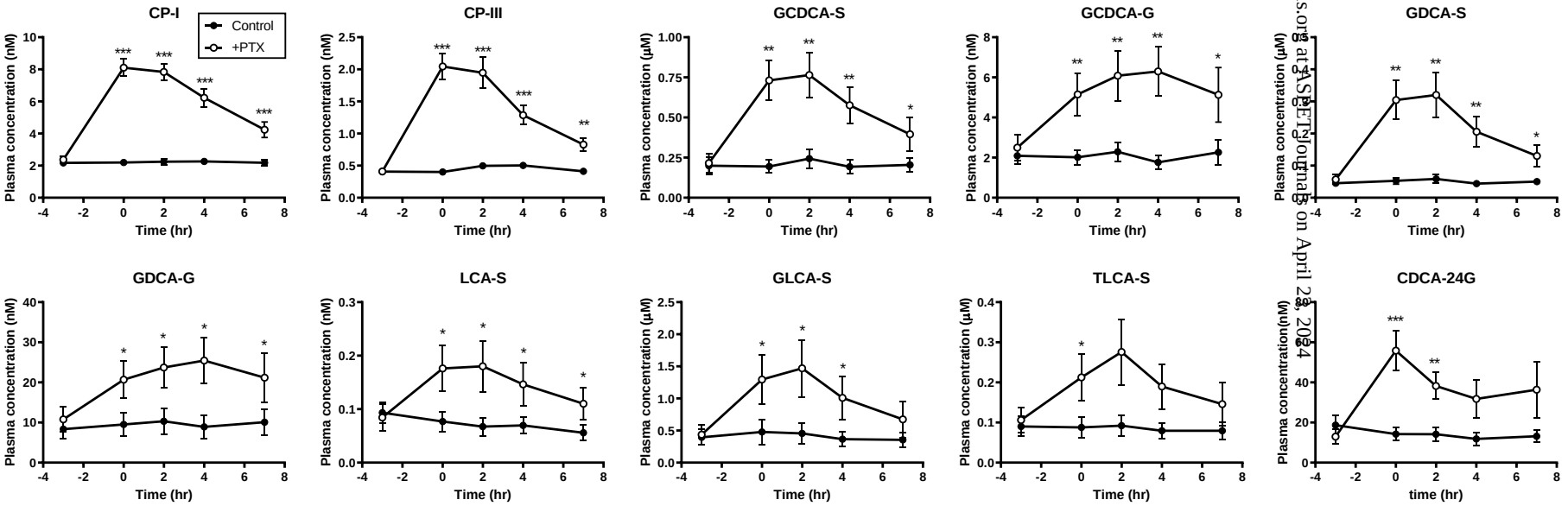

**Figure 4**

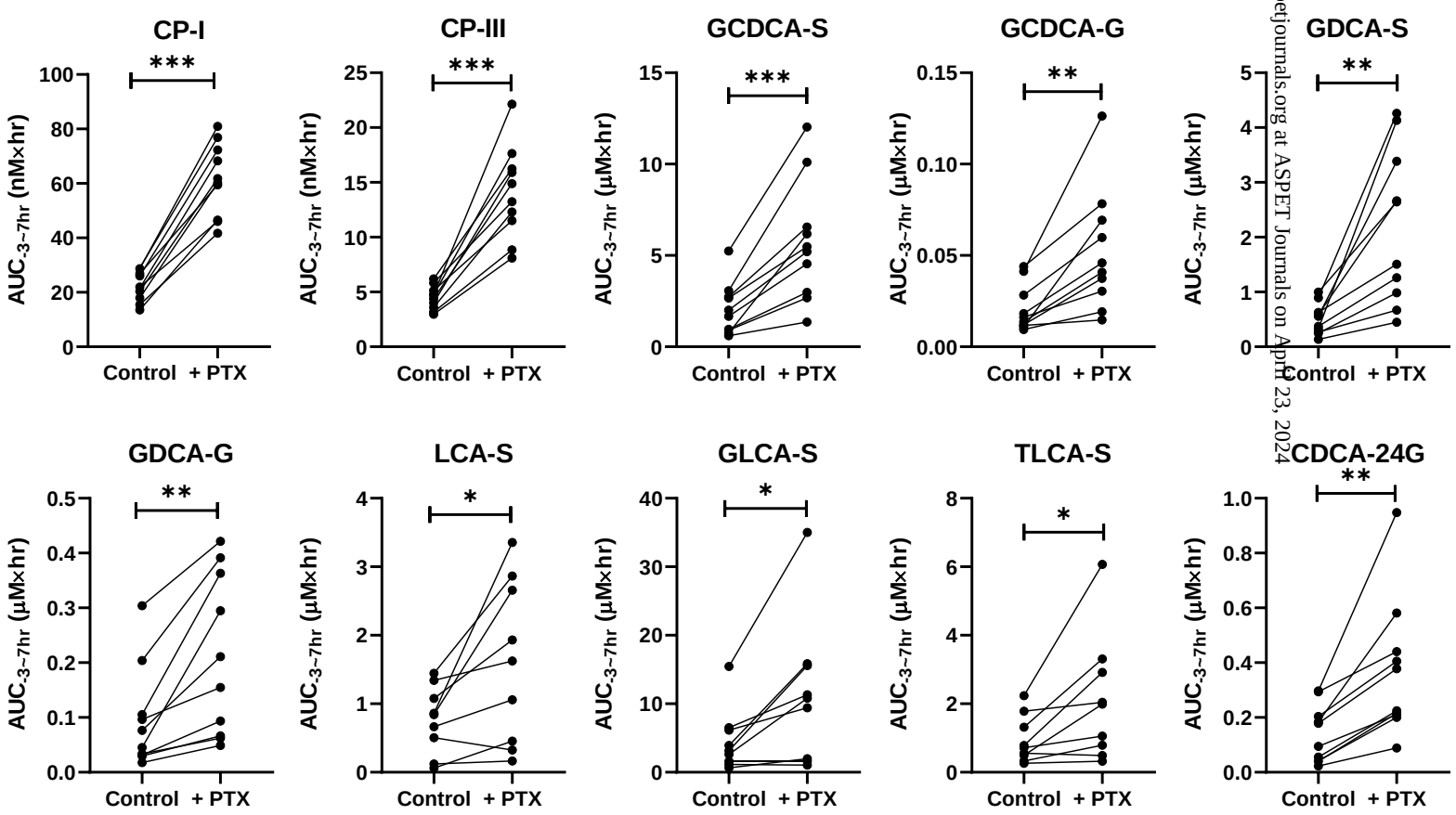

# Figure 5